Stability of Inclined Strip Anchors in Purely Cohesive Soil

R. S. Merifield[1]; A. V. Lyamin[2]; and S. W. Sloan[3]

Abstract: Soil anchors are commonly used as foundation systems for structures requiring uplift resistance such as transmission towers, or for structures requiring lateral resistance, such as sheet pile walls. To date, most anchor studies have been concerned with either the vertical or horizontal uplift problem. In many instances, anchors are placed at inclined orientations depending on the type of application and loading (e.g., transmission tower foundations). However, the important effect of anchor inclination has received very little attention by researchers. This paper applies numerical limit analysis and displacement finite-element analysis to evaluate the stability of inclined strip anchors in undrained clay. Results are presented in the familiar form of breakout factors based on various anchor geometries.

DOI: 10.1061/(ASCE)1090-0241(2005)131:6(792)

CE Database subject headings: Anchors; Pull-out resistance; Finite elements; Limit analysis; Clays; Cohesive soils.

Introduction and Background

During the last 30 years various researchers have proposed approximate techniques to estimate the uplift capacity of soil anchors. The majority of past research has been experimentally based and, as a result, current design practices are largely based on empiricism. In contrast, very few rigorous numerical analyses have been performed to determine the ultimate pullout load of anchors. A comprehensive overview on the topic of strip anchors in clay is given by Merifield et al. (2001) and will not be repeated here.

To date, most anchor studies have been concerned with either the vertical or horizontal pullout problem. In many instances, anchors are placed at inclined orientations depending on the type of application and loading (e.g., transmission tower foundations). However, the important effect of anchor inclination has received very little attention by researchers. A limited number of results for the capacity of inclined square and strip anchors can be found in the works of Meyerhof (1973). The study of Das and Puri (1989) appears to be the most significant attempt to quantify the capacity of inclined anchors. In their tests, the capacity of shallow square anchors embedded in compacted clay with an average undrained shear strength of 42.1 kPa was investigated. Pullout tests were conducted on anchors at inclinations ranging between 0° (horizontal) and 90° (vertical) for embedment ratios (H/B) of up to four. A simple empirical relationship was suggested for predicting the capacity of square anchors at any orientation which compared reasonably well with the laboratory observations. Das and Puri (1989) also concluded that anchors with aspect ratios (L/B) of 5 or greater would, for all practical purposes, behave as a strip anchor.

The purpose of this paper is to take full advantage of the ability of recent numerical formulations of the limit theorems to bracket the actual collapse load of inclined anchors accurately from above and below. The lower and upper bounds are computed, respectively, using the numerical techniques developed by Lyamin and Sloan (2002) and Sloan and Kleeman (1995). In addition, the displacement finite-element formulation presented by Abbo (1997) and Abbo and Sloan (2000) has also been used for comparison purposes. This research software, named *SNAC (Solid Nonlinear Analysis Code)*, was developed with the aim of reducing the complexity of elastoplastic analysis by using advanced solution algorithms with automatic error control. The resulting formulation greatly enhances the ability of the finite-element technique to predict collapse loads accurately and avoids many of the locking problems discussed by Toh and Sloan (1980) and Sloan and Randolph (1982).

Problem of Inclined Anchor Capacity

Problem Definition

The problem geometry to be considered is shown in Fig. 1. An inclined anchor will be defined as an anchor placed at an angle β to the vertical [Fig. 1(b)]. A horizontal anchor is one where $\beta=0°$ [Fig. 1(a)] while a vertical anchor is one where $\beta=90°$ [Fig. 1(c)]. The direction of pullout is perpendicular to the anchor face and the depths H', H_a, and H are, respectively, the depths to the top, middle, and bottom of the anchor from the soil surface. The capacity of anchors inclined at $\beta=22.5$, 45, and 67.5° will be investigated.

A typical lower bound mesh for the problem of an inclined anchor ($\beta=45°$), along with the applied stress boundary conditions, is shown in Fig. 2. The results of the anchor analyses presented are for a perfectly rough rigid anchor. For the lower bound, this is achieved by assuming the individual normal stresses at element nodes on the soil/anchor boundary are unrestricted in magnitude. In the upper bound case, a uniform velocity is prescribed for all the nodes along the anchor. The layout of the upper

[1]Dept. of Agricultural, Civil and Environmental Engineering, Univ. of Southern Queensland, QLD 4350, Australia.

[2]Dept. of Civil, Surveying and Environmental Engineering, The Univ. of Newcastle, NSW 2308, Australia.

[3]Dept. of Civil, Surveying and Environmental Engineering, The Univ. of Newcastle, NSW 2308, Australia.

Note. Discussion open until November 1, 2005. Separate discussions must be submitted for individual papers. To extend the closing date by one month, a written request must be filed with the ASCE Managing Editor. The manuscript for this paper was submitted for review and possible publication on March 26, 2004; approved on November 30, 2004. This paper is part of the ***Journal of Geotechnical and Geoenvironmental Engineering***, Vol. 131, No. 6, June 1, 2005. ©ASCE, ISSN 1090-0241/2005/6-792–799/$25.00.

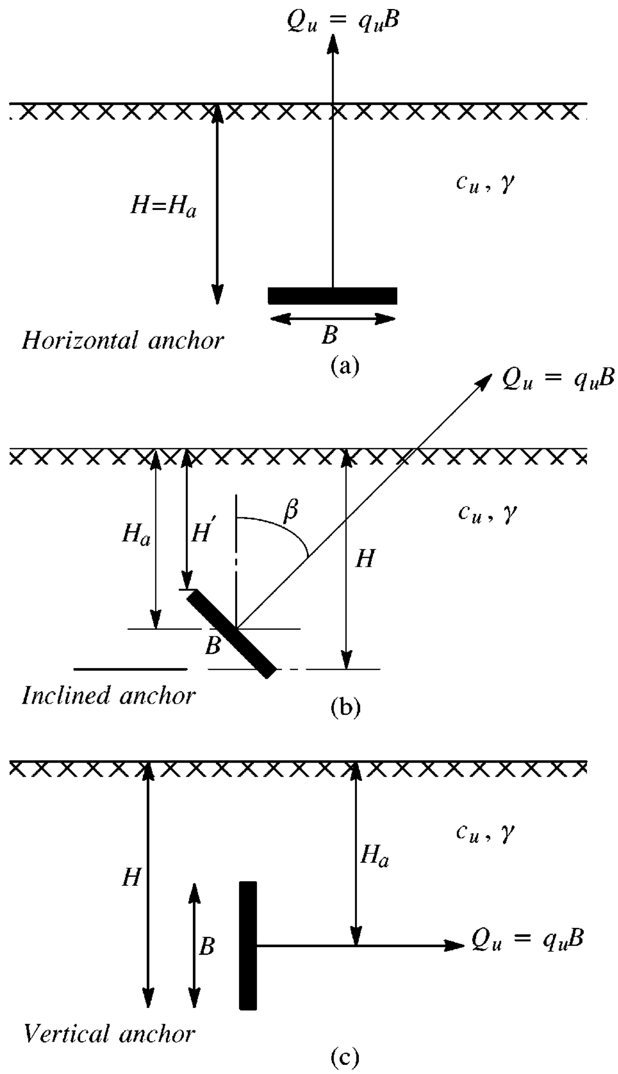

Fig. 1. Problem notation for inclined plate anchors

bound mesh was similar to that of the lower bound. The overall upper bound and lower bound mesh dimensions were selected such that they adequately contained the computed stress field (lower bound) or velocity/plastic field (upper bound). In addition, in order to be a strict lower bound, extension elements were used in the lower bound analyses. For the displacement finite-element (*SNAC*) analyses, between 200 and 400 15 noded triangular elements (1,500–4,000 nodes) were used depending on the problem geometry. Checks were made to ensure the overall *SNAC* mesh dimensions were adequate to contain the zones of plastic shearing and the observed displacement fields.

After Rowe and Davis (1982), the analysis of anchor behavior can be divided into two distinct categories, namely, those of "immediate breakaway" and "no breakaway." In the immediate breakaway case it is assumed that the soil/anchor interface cannot sustain tension so that, upon loading, the vertical stress immediately below the anchor reduces to zero and the anchor is no longer in contact with the underlying soil. This represents the case where there is no adhesion or suction between the soil and anchor. In the no breakaway case the opposite is assumed, with the soil/anchor interface sustaining adequate tension to ensure the anchor remains in contact with the soil at all times. This models the case where an adhesion or suction exists between the anchor and the soil. In reality, it is likely that the true breakaway state will fall somewhere between the extremities of the immediate breakaway and no breakaway cases.

The suction force developed between the anchor and soil is likely to be a function of several variables including the embedment depth, soil permeability, undrained shear strength, and loading rate. As such, the actual magnitude of any adhesion or suction force is highly uncertain and therefore should not be relied upon in the routine design of anchors. For this reason, the anchor analyses presented in this paper are performed for the immediate breakaway case only. This will result in conservative estimates of the actual pullout resistance.

Anchors in Purely Cohesive Soil

The ultimate anchor pullout capacity of horizontal and vertical anchors in purely cohesive soil is usually expressed as a function of the undrained shear strength in the following form (Merifield et al. 2001):

$$q_u = \frac{Q_u}{A} = c_u N_c \tag{1}$$

where for a homogeneous soil profile

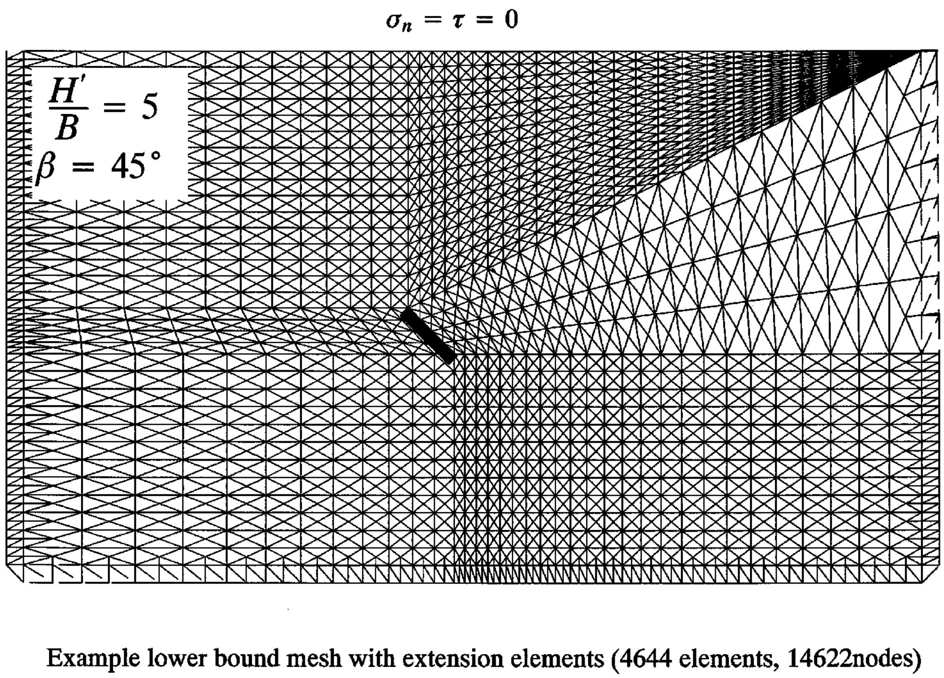

Fig. 2. Example lower bound mesh details

$$N_c = \left(\frac{q_u}{c_u}\right)_{\gamma\neq 0} = N_{co} + \frac{\gamma H_a}{c_u} \tag{2}$$

and the term N_{co} is defined as

$$N_{co} = \left(\frac{q_u}{c_u}\right)_{\gamma=0} \tag{3}$$

In the above, c_u=undrained soil strength and N_c is known as the anchor breakout factor. Note that $H_a=H$ for horizontal anchors [Fig. 1(a)] and $H_a=H-B/2$ for vertical anchors [Fig. 1(c)].

Implicit in Eq. (1) is the assumption that the effects of soil unit weight and cohesion are independent of each other and may be superimposed. It was shown by Merifield et al. (2001) that this assumption generally provides a good approximation to the behavior of anchors in purely cohesive undrained clay.

For an inclined anchor in purely cohesive soil, the ultimate capacity will be given by Eq. (1) where

$$N_c = N_{co\beta} + \frac{\gamma H_a}{c_u} \tag{4}$$

and a new breakout factor $N_{co\beta}$ is introduced which has a value somewhere between the breakout factors N_{co} given in Eq. (3) for vertical and horizontal anchors. Only the homogeneous case is considered.

It should be noted that the breakout factor N_c given in Eq. (4) does not continue to increase indefinitely, but reaches a limiting value which marks the transition between shallow and deep anchor behavior. This process is explained in greater depth by Rowe (1978) and Merifield et al. (2001). The limiting value of the breakout factor is defined as N_{c^*} for a homogeneous soil profile (Merifield et al. 2001).

Results and Discussion

The computed upper and lower bound estimates of the anchor breakout factor $N_{co\beta}$ [Eq. (4)] for homogeneous soils with no soil weight are shown graphically in Figs. 3(a–c). Sufficiently small error bounds were achieved with the true value of the anchor break-out factor typically being bracketed to within ±7%. The greatest variation between the bounds solutions occurs at small embedment ratios ($H_a/B \leqslant 2$) where the error bounds grow to a maximum of ±10%. Also shown in Figs. 3(a–c) are the *SNAC* results. These results plot close to the upper bound solution and are typically within ±5%.

The variation of breakout factor with angle of inclination is clearly presented in Fig. 4. In this figure, the breakout factor is presented as a ratio of the breakout factor for an inclined anchor to that of a vertical anchor. This ratio is defined as the inclination factor i according to

$$i = \frac{N_{co\beta}}{N_{co90}} \tag{5}$$

where i=inclination factor, $N_{co\beta}$=breakout factor for an inclined anchor at an embedment ratio of H_a/B [Figs. 3(a–c)], and N_{co90} =break-out factor for a vertical anchor at the same embedment ratio H_a/B given by

$$N_{co90} = N_{co(\beta=90,H/B=H_a/B+0.5)}$$

The value of the breakout factor N_{co90} can, with sufficient accuracy, be approximated by the following expression (Merifield et al. 2001):

$$N_{co90} = N_{co} = 2.46 \ln\left(2\frac{H}{B}\right) + 0.89 \text{ lower bound} \tag{6}$$

The inclination factor can be seen to increase in a nonlinear manner with increasing inclination from $\beta=0$ to 90°. This observation

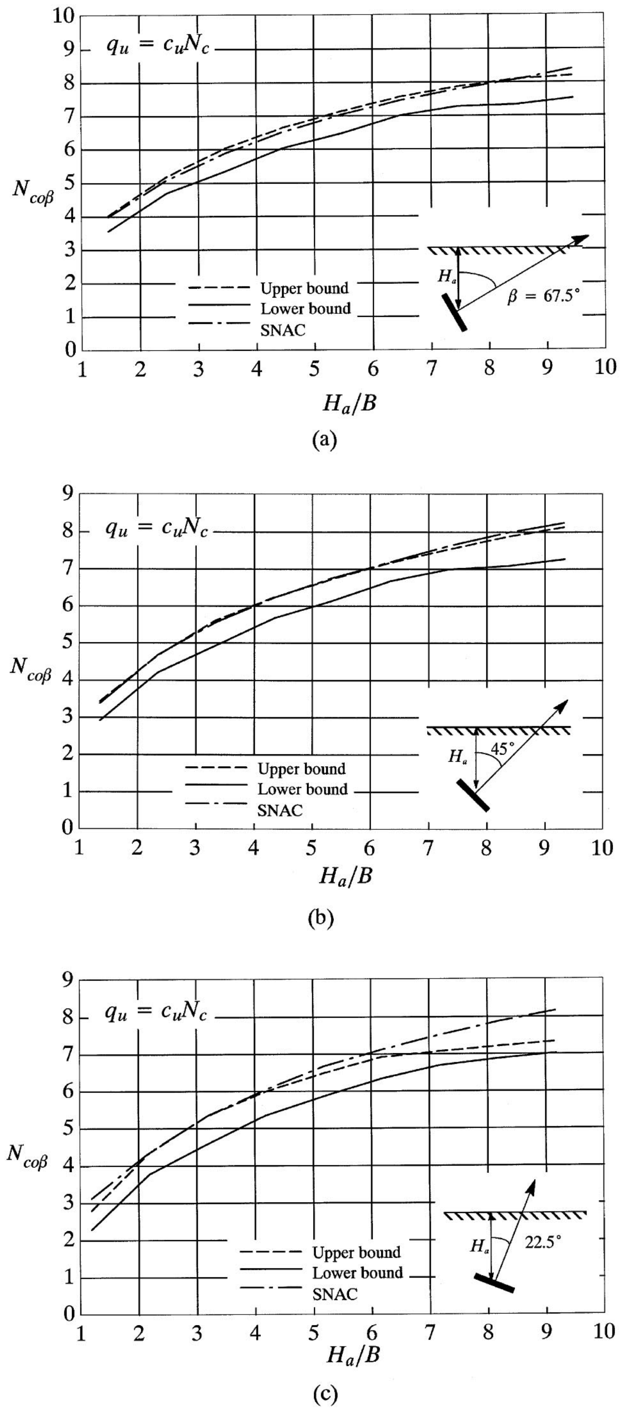

Fig. 3. Breakout factors for inclined anchors in purely cohesive weightless soil

is consistent with the laboratory study of Das and Puri (1989). Fig. 4(a) also suggests that there is very little difference between the capacity of a horizontal anchor ($\beta = 0°$) and anchors inclined at $\beta \leqslant 22.5°$. The greatest rate of increase in anchor capacity appears to occur once $\beta \geqslant 30°$.

The failure mechanisms observed for inclined anchors are illustrated by the upper bound velocity diagrams and *SNAC* displacement plots in Figs. 5–7. As expected, the vector and displacement fields obtained from both types of analyses are very similar. A comparison is shown for anchors at $H'/B = 1$ in Fig. 5.

The lateral extent of surface deformation increases with in-

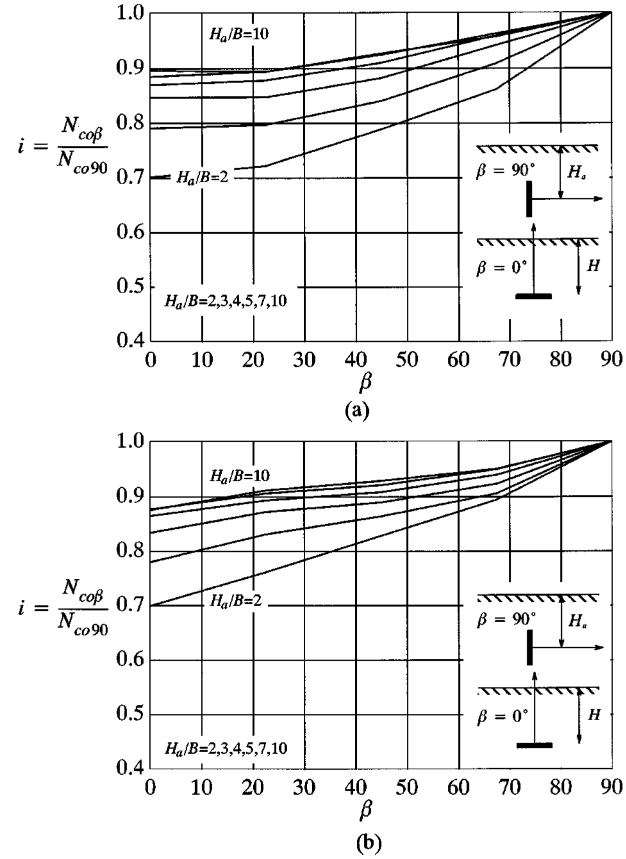

Fig. 4. Inclination factors for anchors in purely cohesive weightless soil: (a) lower bound and (b) *Solid Nonlinear Analysis Code*

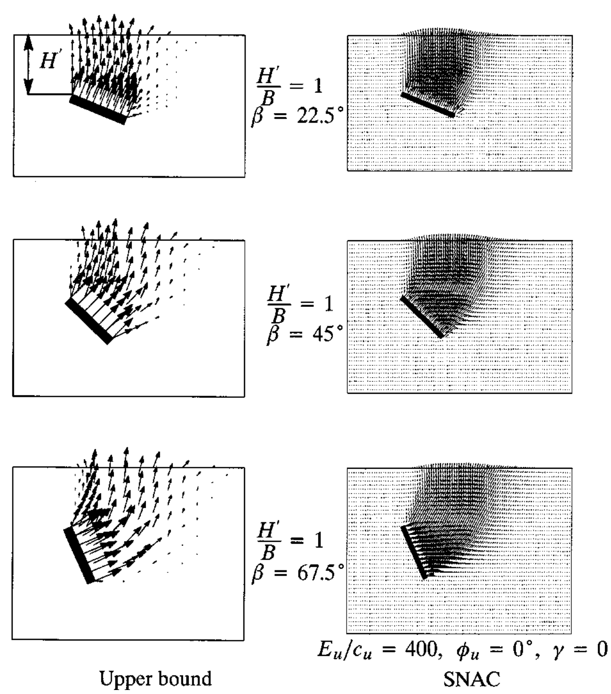

Fig. 5. Failure modes for inclined anchors in purely cohesive weightless soil

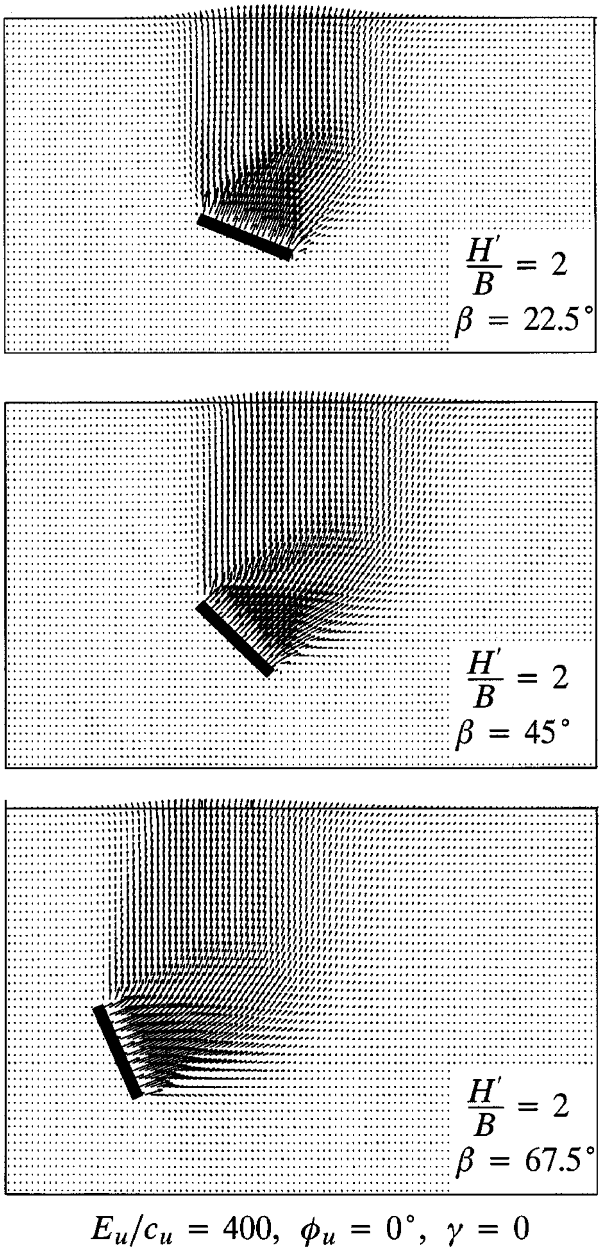

Fig. 6. Failure modes for inclined anchors in purely cohesive weightless soil (*Solid Nonlinear Analysis Code*)

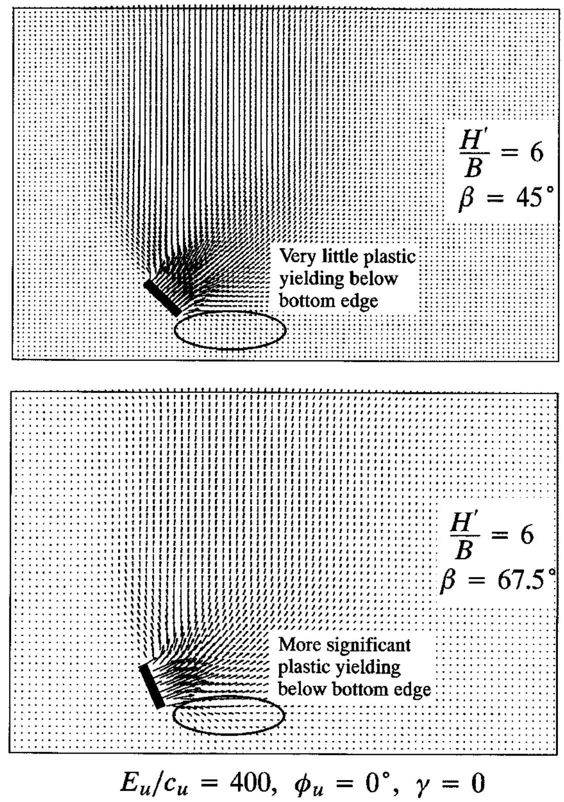

Fig. 7. Failure modes for inclined anchors in purely cohesive weightless soil (*Solid Nonlinear Analysis Code*)

creasing embedment depth and inclination angle. This is consistent with the findings for both the horizontal and vertical anchor cases (Merifield et al. 2001). As expected, the actual magnitude of the surface deformations decreases with the embedment ratio.

Localized elastic zones were observed near the soil surface at most embedment ratios and inclination angles. Several of these zones are shown in Fig. 8 for anchors at $H'/B=4$. In addition, very little plastic shearing was observed below the bottom edge of anchors inclined at $\beta < 45°$. This is highlighted in Fig. 7.

The only laboratory investigation to determine the effect of anchor inclination was by Das and Puri (1989). Unfortunately, these tests were limited to square anchors and their results cannot be compared directly to those presented here. Das and Puri (1989) proposed a simple empirical relationship, based on their laboratory findings, for estimating the capacity of inclined anchors. This relationship is of the form

$$N_{co\beta} = N_{co(\beta=0°)} + [N_{co(\beta=90°)} - N_{co(\beta=0°)}]\left(\frac{\beta°}{90}\right)^2 \tag{7}$$

where N_{co} is obtained at the same value of H_a for each inclination angle β. The value of $N_{co(\beta=0)}$ is the breakout factor for a horizontal anchor and can, with sufficient accuracy, be approximated by the following expression (Merifield et al. 2001)

$$N_{co(\beta=0)} = N_{co} = 2.56 \ln\left(2\frac{H}{B}\right) \text{ lower bound} \tag{8}$$

Out of curiosity, Eq. (7) has been used to estimate the breakout factors for strip anchors and a comparison between these estimates and the results from the current study are shown in Fig. 9. The limit analysis and *SNAC* results (90 points) for inclination angles of 22.5°,45°,67.5° and embedment depths of H_a/B of 1–10 are shown. Fig. 9 indicates that although the empirical equation of Das and Puri (1989) was specifically proposed for inclined square anchors, it also provides a reasonable estimate for the capacity of inclined strip anchors. Eq. (7) plots almost central to the data and, on average, the estimated values are within ±5% of the actual values. This is considered an adequate level of accuracy for design purposes. The discrepancy between the predicted and actual breakout factors tends to be marginally larger for smaller embedment ratios ($H/B \leqslant 2$) where the predicted value is expected to be slightly conservative. It is therefore concluded that the empirical relation given by Eq. (7) may be used to estimate the load capacity of inclined strip anchors.

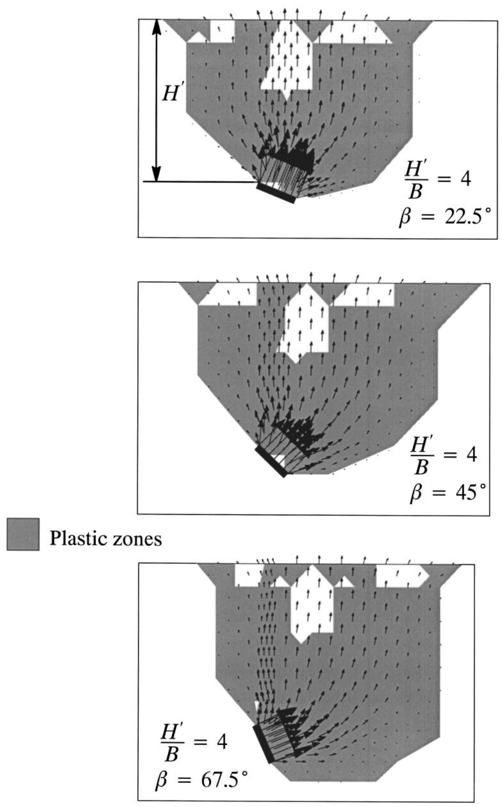

Fig. 8. Failure modes and zones of plastic yielding for inclined anchors in purely cohesive weightless soil (upper bound)

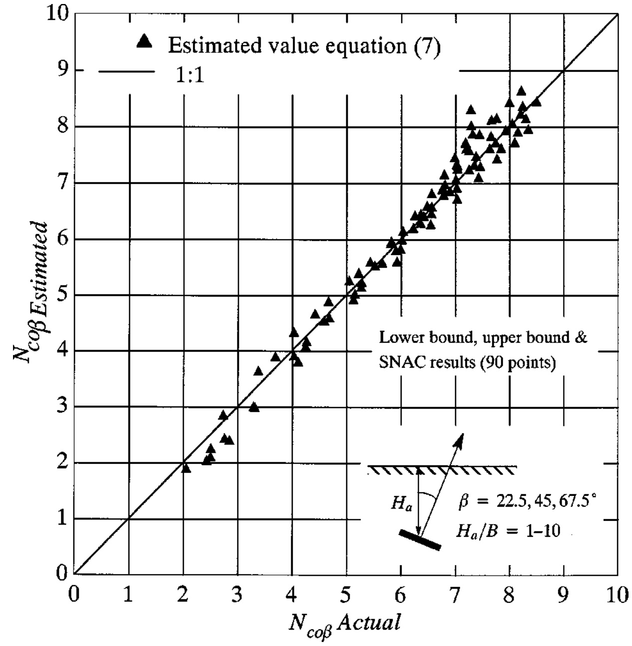

Fig. 9. Comparison of breakout factors for inclined strip anchors in purely cohesive weightless soil

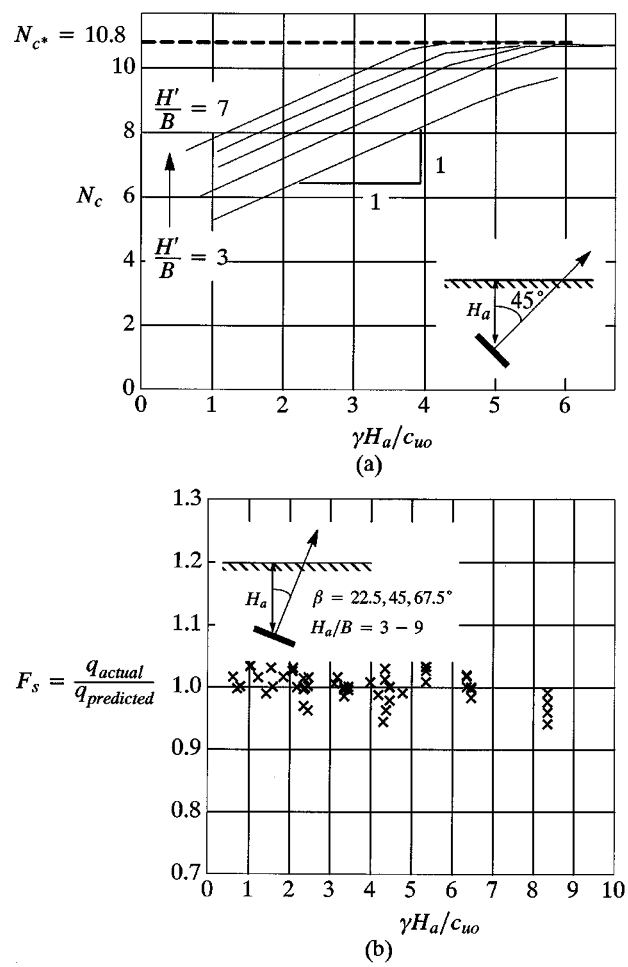

Fig. 10. Effect of overburden pressure for inclined anchors in purely cohesive soil—Lower bound

Effect of Overburden Pressure

The numerical results discussed above are limited to soil with no unit weight, and therefore the effect of soil weight (overburden) needs to be investigated. If our assumption of superposition is valid then it would be expected that the ultimate anchor capacity, as given by Eqs. (1) and (2), would increase linearly with the dimensionless overburden pressure $\gamma H_a/c_u$. The results from further lower bound analyses that include cohesion and soil weight, shown in Fig. 10(a), confirm that this is indeed the case. This conclusion is in agreement with the observations of Rowe (1978) and Merifield et al. (2001).

The error due to superposition can be expressed in the following form:

$$F_s = \frac{q_{\text{actual}}}{q_{\text{predicted}}} \tag{9}$$

and is shown in Fig. 10(b). This figure indicates that the superposition error is likely to be insignificant.

Fig. 10(a) indicates that the ultimate anchor capacity increases linearly with overburden pressure up to a limiting value. This limiting value reflects the transition of the failure mode from being a nonlocal one to a local one. An example of a "deep" anchor failure is shown by the velocity diagram in Fig. 11 for an anchor where $\beta=45°$. At a given embedment depth the anchor failure mode may be nonlocalized or localized, depending on the dimensionless overburden ratio $\gamma H_a/c_u$. For shallow anchors exhibiting nonlocalized failure, the mode of failure is independent of the overburden pressure.

For deep anchors, the average limiting values of the breakout factor N_{c^*} for all values of β were found to be 10.8 (lower bound)

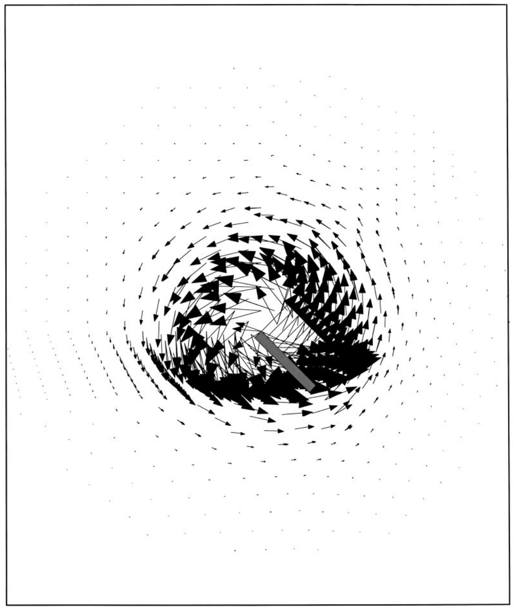

Fig. 11. Upper bound failure mechanism for a deep inclined anchor, $\beta=45°$

and 11.96 (upper bound). These values sit somewhere between the values obtained by Merifield et al. (2001) for deep horizontal and vertical anchors and compare well with the analytical solutions of Rowe (1978), who found lower and upper bounds of 10.28 and 11.42 for the horizontal anchor case. Intuitively, the value of N_{c^*} should, for a comparable mesh density, be independent of β. Unfortunately, successfully bracketing the collapse load for a deep anchor (N_{c^*}) proved difficult and very much mesh dependent. For deep anchors, the form of the velocity field at collapse is essentially independent of the overburden pressure.

Suggested Procedure for Estimation of Uplift Capacity

1. Determine representative values of the material parameters c_u and γ.
2. Knowing the anchor size B and embedment depth H_a calculate the embedment ratio H_a/B and overburden ratio $\gamma H_a/c_u$.
3. Calculate N_{co90} using Eq. (6) with $H/B=H_a/B+0.5$.
4. *a.* For an anchor at $\beta=22.5$, 45, or 67.5°, estimate the breakout factor N_{co} using Figs. 3(a–c), depending on the anchor orientation.
   b. For anchors at other orientations, estimate the anchor inclination factor i using Fig. 4(a) and the value of H_a/B obtained in Eq. (3). Then calculate N_{co} as per Eq. (5). A value of N_{co} could also be estimated from Eq. (7) using Eqs. (6) and (8).
5. Adopt $N_{c^*}=10.8$.
6. *a.* Calculate the breakout factor N_c using Eq. (2).
   b. If $N_c \geqslant N_{c^*}$ then the anchor is a deep anchor. The ultimate pullout capacity is given by Eq. (1) where $N_c=N_{c^*}=10.8$.
   c. If $N_c \leqslant N_{c^*}$ then the anchor is a shallow anchor. The ultimate pullout capacity is given by Eq. (1) where N_c is the value obtained in 6.*a*.

Example of Application

We now illustrate how to use the results presented to determine the ultimate pullout capacity of an inclined anchor in clay.

Problem: A plate anchor of width 0.2 m is to be embedded at $H_a=1.5$ m at an orientation of 45°. Determine the ultimate pullout capacity given that the clay has a shear strength $c_u=50$ kPa and unit weight $\gamma=15$ kN/m^3.

The systematic procedures given above will now be used to determine the ultimate anchor capacity.

1. Given $c_u=50$ kPa and $\gamma=15$ kN/m^3;
2. The embedment ratio can be calculated as $H_a/B=1.5/0.2=7.5$; The dimensionless parameter $\gamma H_a/c_u=(15\times1.5)/50=0.45$;
3. $N_{co90}=2.46\ln(2H/B)+0.89=2.46\ln[2(7.5+0.5)]+0.89=7.71$;
4. *a*. From Fig. 3, $N_{co}=7$ (lower bound);
5. Adopt $N_{c^*}=10.8$;
6. *a*. From Eq. (2), $N_c=7+0.45=7.45$;
   b. $N_c<N_{c^*}$ and therefore the anchor is "shallow" and using Eq. (1)

$$q_u = c_uN_c = 50 \times 7.45 = \mathbf{372.5\ kPa}$$

$$Q_u = 375.2 \times (0.2) = \mathbf{74.5\ kN}\ \textit{per m run}$$

Direct finite-element lower bound calculations using these parameters gives $q_u=370.6$ kPa, which is 0.5% less than that obtained above using the suggested procedure.

Conclusions

A rigorous numerical study into the ultimate capacity of inclined strip anchors has been presented. Consideration has been given to the effect of embedment depth and anchor inclination. The results have been presented as breakout factors in chart form to facilitate their use in solving practical design problems.

The following conclusions can be drawn from the results presented in this paper.

1. Using the lower and upper bound limit theorems, small error bounds of less than ±7% were achieved on the true value of the breakout factor for anchors inclined at 22.5, 45, and 67.5° to the vertical in a weightless soil.
2. The displacement finite-element (*SNAC*) results compare favorably with the numerical bounds solutions, and are typically within ±5% of the upper bound solutions.
3. The effect of anchor inclination on the pullout capacity of anchors has been investigated. A simple empirical equation has been proposed which, on average, provides collapse load estimates within ±5% of the actual values.
4. The ultimate anchor capacity increases linearly with overburden pressure up to a limiting value that reflects the transition from a nonlocalized to localized (or "deep") failure mechanism.

Notation

The following symbols are used in this paper:

A = anchor area;
B = anchor width;
c_u = soil cohesion;

D = anchor diameter;
E_u = undrained Young's modulus;
H = anchor embedment depth;
H', H_a = depth to top and middle of anchor;
H/B = anchor embedment ratio;
H/D = anchor embedment ratio;
i = anchor inclination factor;
L = anchor length;
L/B = anchor aspect ratio;
N_c = anchor break-out factor;
N_{co} = anchor break-out factor for weightless soil;
$N_{co\beta}$ = break-out factor for inclined anchor in weightless soil;
N_{co90} = anchor break-out factor for a vertical anchor;
q_u = ultimate anchor pullout capacity;
S_F = dimensionless anchor shape factor;
β = anchor inclination angle;
γ = soil unit weight; and
ϕ_u = soil friction angle.

References

Abbo, A. J. (1997). "Finite element algorithms for elastoplasticity and consolidation." PhD thesis, Department of Civil, Surveying and Environmental Engineering, University of Newcastle, NSW.

Abbo, A. J., and Sloan, S. W. (2000). *SNAC users manual Version 2.0*.

Das, B. M., and Puri, V. K. (1989). "Holding capacity of inclined square plate anchors in clay." *Soils Found.*, 29(3), 138–144.

Lyamin, A. V., and Sloan, S. W. (2002). "Lower bound limit analysis using non-linear programming." *Int. J. Numer. Methods Eng.*, 55(5), 573–611.

Merifield, R. S., Sloan, S. W., and Yu, H. S. (2001). "Stability of plate anchors in undrained clay." *Geotechnique*, 51(2), 141–153.

Meyerhof, G. G. (1973). "Uplift resistance of inclined anchors and piles." *Proc., 8th Int. Conf. on Soil Mechanics and Foundation Engineering, Moscow*, Vol. 2, 167–172.

Rowe, R. K. (1978). "Soil structure interaction analysis and its application to the prediction of anchor behaviour." PhD thesis, University of Sydney, Australia.

Rowe, R. K., and Davis, E. H. (1982). "The behaviour of anchor plates in clay." *Geotechnique*, 32(1), 9–23.

Sloan, S. W., and Kleeman, P. W. (1995). "Upper bound limit analysis using discontinuous velocity fields." *Comput. Methods Appl. Mech. Eng.*, 127, 293–314.

Sloan, S. W., and Randolph, M. F. (1982). "Numerical prediction of collapse loads using finite element methods." *Int. J. Numer. Analyt. Meth. Geomech.*, 6(1), 47–76.

Toh, C. T., and Sloan, S. W. (1980). "Finite element analysis of isotropic and anisotropic cohesive soils with a view to correctly predicting impending collapse." *Int. J. Numer. Analyt. Meth. Geomech.*, 4, 1–23.